Formation, Reactivity, and Proposed Structures of Gas-Phase Triosmium Cluster Ions: $H_2Os_3(CO)_{10}^+$ and Its Dimers, Trimers, and Fragments

Steven L. Mullen[†,§] and Alan G. Marshall*[†,‡]

Contribution from the Department of Chemistry and Department of Biochemistry, The Ohio State University, Columbus, Ohio 43210. *Received June 12, 1987*

Abstract: Electron ionization of $H_2Os_3(CO)_{10}$ vapor in a Fourier transform ion cyclotron resonance mass spectrometer produces abundant $H_2Os_3(CO)_x^+$ ions, with $0 \leq x \leq 10$. By means of mass-selective stored-waveform ejection, individual ionic species may be isolated, and their condensation with neutral parent molecules can be shown to occur with the elimination of two to three carbonyls per stage, to produce Os_6, Os_9, Os_{12}, and Os_{15} cluster ion species. For a given structure and number of bonds, a discontinuity in average osmium electron deficiency between the observed triosmium dimers, $H_2Os_6(CO)_{14}^+$ and $Os_6(CO)_{13}^+$, and between the observed trimers, $H_2Os_9(CO)_{20}^+$ and $Os_9(CO)_{19}^+$, is predicted. However, kinetics measurements show a continuous variation in reactivity with number of carbonyls for both the dimers and trimers. Therefore, the results imply a change in the number of bonds, either by a change in structure or by an increase in the number of Os–Os double bonds. By analogy to known structures of neutral $H_2Os_6(CO)_{18}$ and $Os_6(CO)_{18}$, we propose capped square-pyramidal and bicapped tetrahedral structures for dimers with and without hydrogens. A tricapped ($\square^3$) trigonal-prismatic structure is suggested for trimers possessing $\geq$20 carbonyls, and a tricapped octahedral structure is suggested for trimers with $\leq$19 carbonyls. In the absence of relevant X-ray structural data for homologous trimer neutrals, the formation of Os–Os double bonds on loss of hydrogens is possible but unlikely, since large osmium clusters are not known to contain such bonds. An electron deficiency much greater than 2 is avoided in the trimers, in which the electron deficiency is lowered by the addition of hydrogens.

This paper extends to the heavier transition metals (in this case, osmium) the Fourier transform ion cyclotron resonance (FT/ICR) mass spectrometry/mass spectrometry (MS/MS) determination of metal cluster ion–molecule condensation reaction pathways and kinetics. Because of the high mass and multiple isotopes for Os_n clusters (n = 3, 6, 9, ...), isolation of a species having a single chemical formula requires a new and more selective ion-ejection technique in the first stage of the MS/MS experiment. To that end, this paper describes the first chemical application of our recently developed stored-waveform technique for high-resolution ion ejection. Once the desired ions have been isolated, we can proceed to determine the ion–molecule pathways and rate constants, from which metal cluster molecular structures can be inferred.

Transition-Metal Cluster Carbonyls. $H_2Os_3(CO)_{10}$ was first synthesized by Johnson et al.[1] in 1968 and is often used as a starting material for the synthesis of larger clusters,[2-4] many of which have recently been cataloged.[5] Transition-metal clusters (particularly of the osmium family) are currently of interest as potential catalysts[6] as well as for their intrinsic interest as an intermediate state between individual molecules and bulk matter. The determination of structure and bonding in such clusters is an active research area, because the rates of simple reactions on the surfaces of small metal clusters have been shown to depend on the number of metal atoms in the cluster (e.g., dissociative chemisorption of molecular hydrogen and deuterium on Co and Nb clusters of 1–20 metal atoms).[7] Unfortunately, relatively few of the larger osmium clusters have been crystallized for structure determination by X-ray diffraction. Even less is known about the possible structures of gas-phase osmium cluster ions. In this paper, we describe the generation and self-reactivity of triosmium cluster cations with their parent neutrals to form cluster ions containing up to 15 osmium atoms, and we offer kinetic evidence for the structures of triosmium dimer and trimer cations. The instrumental techniques and reasoning in this work are modeled after those originally developed by Ridge and co-workers for other transition-metal cluster ions.[8,9]

Gas-phase ion–molecule clustering reactions of transition-metal carbonyls were first seen in 1966[10] and metal carbonyl complexes by FT/ICR in 1980.[11] Early studies described clustering of $Fe(CO)_5$,[12,13] $Ni(CO)_4$,[14] $Cr(CO)_6$,[15,16] and $CoNO(CO)_3$.[17] Recently, Wronka and Ridge[18] formed cluster anions as large as $Fe_4(CO)_{13}^-$ by allowing negative daughter ions of $Fe(CO)_5$ to react with the parent neutral in a scanning ion cyclotron resonance mass spectrometer and were able to relate electron deficiency to the number of double bonds in each species. Meckstroth et al.[8,19] formed rhenium carbonyl clusters up to $Re^{10}(CO)_{29}^+$ by self-reacting $Re_2(CO)_{10}$ in an FT/ICR instrument[20] and established a correlation between electron deficiency and ion–molecule reaction relative rate constants for clusters containing various numbers of carbonyls. For clusters having the same number of rhenium atoms, a smaller number of carbonyls resulted in a greater electron

[†] Department of Chemistry.
[‡] Department of Biochemistry.
[§] Present address: Department of Biochemistry, Michigan State University, East Lansing, MI 48824.

(1) Johnson, B. F. G.; Lewis, J.; Kilty, P. A. *J. Chem. Soc. A* **1968**, 2859–2864.
(2) Siriwardane, U. Doctoral Dissertation, The Ohio State University, 1985.
(3) Jan, D. Y. Doctoral Dissertation, The Ohio State University, 1985.
(4) Hsu, L. Y.; Hsu, W. L.; Jan, D. Y.; Shore, S. G. *Organometallics* **1986**, *5*, 1041–1049.
(5) Knox, G. R. *Organometallic Compounds of Ruthenium and Osmium*; Chapman and Hall: London, 1985.
(6) Geusic, M. E.; Morse, M. D.; Smalley, R. E. *J. Chem. Phys.* **1985**, *82*, 590–591.
(7) Gates, B. C. *Stud. Surf. Sci. Catal.* **1986**, *29*, 415–425.
(8) Meckstroth, W. K.; Ridge, D. P.; Reents, W. D., Jr. *J. Phys. Chem.* **1985**, *89*, 612–617.
(9) Meckstroth, W. K.; Freas, R. B.; Reents, W. D., Jr.; Ridge, D. P. *Inorg. Chem.* **1985**, *24*, 3139–3146.
(10) Schumacher, E.; Taubenest, R. *Helv. Chim. Acta* **1966**, *49*, 1447–1455.
(11) Parisod, G.; Comisarow, M. B. *Adv. Mass Spectrom.* **1980**, *8A*, 212–223.
(12) Foster, M. S.; Beauchamp, J. L. *J. Am. Chem. Soc.* **1971**, *93*, 4924–4926.
(13) Foster, M. S.; Beauchamp, J. L. *J. Am. Chem. Soc.* **1975**, *97*, 4808–4814.
(14) Allison, J.; Ridge, D. P. *J. Am. Chem. Soc.* **1979**, *101*, 4998–5009.
(15) Kraihanzel, C. S.; Conville, J. J.; Sturm, J. E. *J. Chem. Soc., Chem. Commun.* **1971**, 159–161.
(16) Allison, J. Doctoral Dissertation, University of Delaware, 1978.
(17) Weddle, G. H.; Allison, J.; Ridge, D. P. *J. Am. Chem. Soc.* **1977**, *99*, 105–109.
(18) Wronka, J.; Ridge, D. P. *J. am. Chem. Soc.* **1984**, *106*, 67–71.
(19) Meckstroth, W. K.; Ridge, D. P. *Int. J. Mass Spectrom. Ion Processes* **1984**, *61*, 149–152.
(20) Marshall, A. G. *Acc. Chem. Res.* **1985**, *18*, 316–322.

0002-7863/88/1510-1766$01.50/0

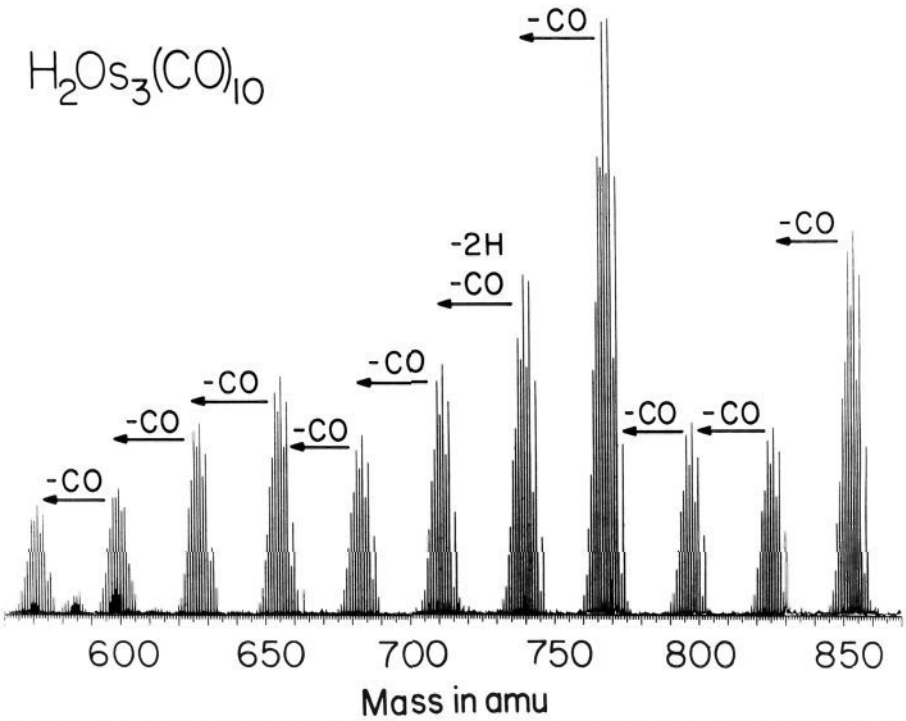

Figure 1. FT/ICR positive-ion mass spectrum of electron-ionized $H_2Os_3(CO)_{10}$, in which the ions are excited and detected immediately after their formation.

deficiency, and the greater the deficiency, the greater the rate constant. Chemical reactivity could then be related to ion structure.

Meckstroth et al. subsequently characterized cluster cations as large as $Mn_8(CO)_{25}^+$, formed by the self-reaction of $Mn_2(CO)_{10}$, and $Re_3Mn_3(CO)_{19}^+$, formed by the self-reaction of $ReMn(CO)_{10}$.[9] Again, chemical reactivity and electron deficiency correlated, provided that ligand crowding and electronic effects such as multiple bonding and ligand-induced restructuring were taken into account. In general, the mixed-metal clusters contained an equal number of manganese and rhenium atoms. Fredeen and Russell[21] later self-reacted $Cr(CO)_6$ and $Fe(CO)_5$ to form cluster cations ranging up to $Cr_4(CO)_{12}^+$ and $Fe_6(CO)_{18}^+$, respectively, and were also able to relate chemical reactivity to electron deficiency. In a subsequent study,[22] Fredeen and Russell characterized $Ni_6(CO)_8^+$ clusters formed from $Ni(CO)_4$ and $Co_6(CO)_{11}^+$ and $Co(CO)_5(NO)_5^+$ formed from $Co(CO)_3(NO)$.

Electron counting for $H_2Os_3(CO)_{10}$ shows that there are 2 less electrons than are required to give 18 to each osmium. The 18-electron valency requirement for osmium can be satisfied either by introduction of an osmium–osmium double bond[23,24] or by multicenter delocalized bonds.[25] As a result of its electron deficiency, $H_2Os_3(CO)_{10}$ in solution reacts readily with 2-electron donors such as CO, $P(C_6H_6)_3$, $P(CH_3)_2(C_6H_6)$, $PCH_3(C_6H_6)_2$,[26] and CNR (R = CH_3, C_6H_6, and t-C_4H_9)[27] to produce simple addition products in which the donor attaches to the osmium atom at one end of an Os–H–Os bridge and the hydrogen migrates to the osmium atom at the other end of the bridge.

Mass Spectrometric Problems and Solutions. Because of osmium's high mass and large number of stable isotopes, the study of large osmium cluster ions by FT/ICR mass spectrometry is experimentally challenging. First, since FT/ICR signal-to-noise ratio and mass resolution vary directly with magnetic field strength,[28] a magnetic field of at least 3 T is required to resolve the isotopic multiplets for such massive clusters. Second, since FT/ICR signal-to-noise ratio varies directly with ICR orbital radius,[29] a trapped-ion cell of a 2-in. radius (rather than the more common 1-in. cell) is desirable. With these capabilities, we can resolve nominal masses even for triosmium trimer cations (i.e., containing Os_9 clusters) at about 2300 amu. Third, the small frequency separation between mass spectral isotopic multiplets at high mass greatly increases the difficulty of mass-selective ion ejection required to isolate ions of a given chemical composition for kinetic measurements. In the present work, stored waveform inverse Fourier transform (SWIFT) excitation[30,31] is applied in place of conventional frequency-sweep excitation to provide superior mass selectivity for double-resonance experiments.[32,33]

Table I. Mass Spectral Parameters

experiment	SWIFT isolation	kinetics
data points	32 768	32 768
no. of scans averaged	100	100
low mass, amu	500	500
high mass, amu	2000	4000
pressure, Torr	9.8×10^{-9}	1.2×10^{-9}
electron beam duration, ms	120	120
electron beam potential, eV	50	50
electron emission current, nA	515	505
trapping potential, V	0.1	0.1
ejection time, ms	235.885	
ejection bandwidth, kHz	~30 (3-kHz window)	
ejection attenuation, dB	5	

(21) Fredeen, D. A.; Russell, D. H. *J. Am. Chem. Soc.* **1985**, *107*, 3762–3768.
(22) Fredeen, D. A.; Russell, D. H. *J. Am. Chem. Soc.* **1986**, *108*, 1860–1867.
(23) Kaesz, H. D. *Chem. Br.* **1973**, 344–352.
(24) Churchill, M. R.; DeBoer, B. G.; Rotella, F. J. *Inorg. Chem.* **1976**, *15*, 1843–1853.
(25) Broach, R. W.; Williams, J. M. *Inorg. Chem.* **1979**, *18*, 314–319.
(26) Shapley, J. R.; Keister, J. B.; Churchill, M. R.; DeBoer, B. G. *J. Am. Chem. Soc.* **1975**, *97*, 4145–4146.
(27) Deeming, A. J.; Hasso, S. *J. Organomet. Chem.* **1976**, *114*, 313–324.
(28) Marshall, A. G.; Comisarow, M. B.; Parisod, G. *J. Chem. Phys.* **1979**, *71*, 4434–4444.
(29) Comisarow, M. B. *J. Chem. Phys.* **1978**, *69*, 4097–4104.
(30) Marshall, A. G.; Wang, T.-C. L.; Ricca, T. L. *J. Am. Chem. Soc.* **1985**, *107*, 7893–7897.
(31) Chen, L.; Wang, T.-C. L.; Ricca, T. L.; Marshall, A. G. *Anal. Chem.* **1987**, *59*, 449–454.
(32) Comisarow, M. B.; Grassi, V.; Parisod, G. *Chem. Phys. Lett.* **1978**, *57*, 413–416.

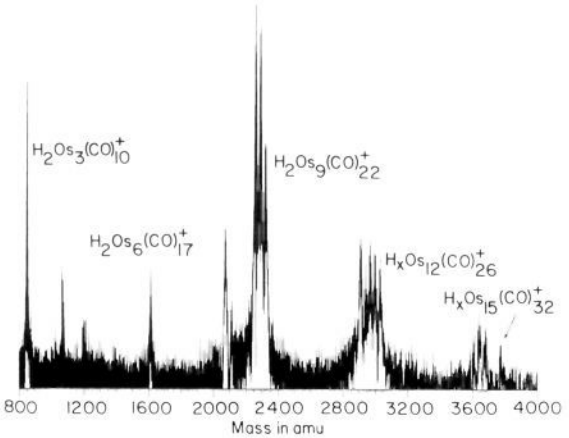

Figure 2. FT/ICR low-resolution positive-ion mass spectrum of the ionic products of the self-reaction of $H_2Os_3(CO)_{10}$ with its molecular and fragment ions for 0.5 s at 6×10^{-7} Torr. Observable product ions include $H_2Os_3(CO)_{10}^+$, $H_2Os_6(CO)_{17}^+$, $H_xOs_9(CO)_{15}^+$ to $H_xOs_9(CO)_{22}^+$, $H_xOs_{12}(CO)_{22}^+$ through $H_xOs_{12}(CO)_{26}^+$, and $H_xOs_{15}(CO)_{27}^+$ to $H_xOs_{15}(CO)_{32}^+$.

Experimental Section

All FT/ICR mass spectra were obtained at 3.0 T with a Nicolet FT/MS-1000 instrument equipped with a 2-in. cubic cell unless otherwise noted. $H_2Os_3(CO)_{10}$, furnished by S. G. Shore, was introduced via a direct-insertion probe heated to approximately 40 °C. Other spectral parameters are listed in Table I for both double-resonance and kinetic experiments. The ion–molecule reaction period for double-resonance studies was 1 s for triosmium dimers and 10 s for triosmium trimers, and for the kinetic studies, the ion–molecule reaction period varied from 500 ms to 16 s.

Results and Discussion

FT/ICR Single-Stage Experiments. The molecular and fragment ions formed by electron ionization of $H_2Os_3(CO)_{10}$ are shown in the FT/ICR mass spectrum of Figure 1. This spectrum was obtained by exciting and detecting the ions essentially immediately after their formation. Mass resolution is sufficient to show the characteristic isotopic multiplet pattern for Os_3 in the molecular and fragment ions corresponding to clusters containing 0–10 carbonyls. It is interesting to note that both hydrogens are lost simultaneously with the fifth carbonyl (see below).

The detection of larger triosmium cluster ions poses an immediate dilemma. On the one hand, the rates of the ion–molecule condensation reactions required to form the larger clusters from (e.g.) the self-reaction of $H_xOs_3(CO)_y^+$ with $H_2Os_3(CO)_{10}$ increase with sample pressure. Thus, *high* pressure is desirable to increase the yield of high-mass product ions. On the other hand, FT/ICR mass resolution varies inversely with pressure,[28] so that *low* pressure is necessary to furnish the high mass resolution needed to resolve ions of different chemical formula in the mass spectrum.

For example, in order to observe condensation reactions up to and including triosmium pentamers (i.e., Os_{15} species) shown in the wide-range FT/ICR mass spectrum of Figure 2, self-reaction of electron-ionized $H_2Os_3(CO)_{10}$ was allowed to proceed for 0.5 s at a pressure of 6×10^{-7} Torr. (In this case, a 1-in. cell and turbomolecular pump were used in place of the 2-in. cell and cryopump for most of the other experiments.) In addition to the triosmium monomer, $H_2Os_3(CO)_{10}^+$, and dimer, $H_2Os_3(CO)_{17}^+$, trimer, $H_xOs_9(CO)_{15}^+$ through $H_xOs_9(CO)_{22}^+$, tetramer, $H_xOs_{12}(CO)_{22}^+$ through $H_xOs_{12}(CO)_{26}^+$, and pentamer, $H_xOs_{15}(CO)_{27}^+$ through $H_xOs_{15}(CO)_{32}^+$, species can be seen. Because of the limited signal-to-noise ratio and insufficient mass resolution within the isotopic multiplets (due to the relatively high pressure and wide mass range), the numbers of hydrogens in the trimer, tetramer, and pentamer could not be determined. It is interesting to note that Meckstroth et al.[8,19] also produced condensation products containing up to pentamers from $Re_2(CO)_{10}$ and Fredeen and Russell[21,22] produced multimers up to hexamers from $Fe(CO)_5$, $Ni(CO)_4$, and $Co(CO)_3(NO)$. We are presumably able to form larger clusters (up to Os_{15} units) because our starting material is itself a metal trimer rather than a monomer or dimer.

(33) Mullen, S. L. Doctoral Dissertation, The Ohio State University, 1987.

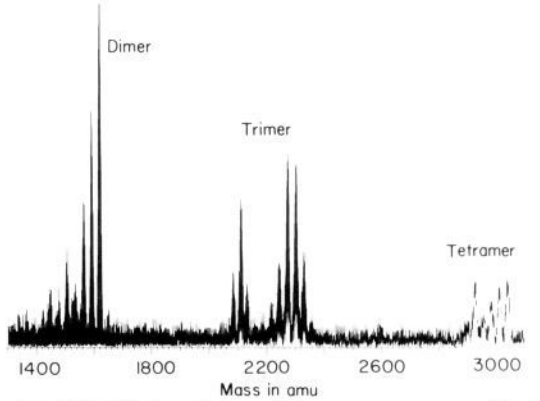

Figure 3. FT/ICR high-resolution positive-ion mass spectrum of the ionic products of the self-reaction of $H_2Os_3(CO)_{10}$ with its molecular and fragment ions for 10.0 s at 1×10^{-9} Torr. The trimer ions range from $H_xOs_9(CO)_{13}^+$ to $H_xOs_9(CO)_{23}^+$, and tetramer ions range from $H_xOs_{12}(CO)_{21}^+$ to $H_xOs_{12}(CO)_{26}^+$.

Analog mass resolution can be increased by reducing the pressure, and digital mass resolution can be increased by reducing the spectral bandwidth. Figure 3 shows FT/ICR mass spectra of the triosmium dimer, trimer, and tetramer cations, obtained at much lower pressure (1×10^{-9} Torr), much longer reaction time (10.0 s), and somewhat reduced mass range. Although the triosmium pentamer is no longer produced at the lower pressure, the remaining mass spectral peaks are much better resolved and clearly show triosmium trimer cations ranging from $H_xOs_9(CO)_{13}^+$ through $H_xOs_9(CO)_{23}^+$ and tetramer cations ranging from $H_xOs_{12}(CO)_{21}^+$ through $H_xOs_{12}(CO)_{26}^+$; many more species can now be resolved (compared to Figure 2).

FT/ICR MS/MS Experiments. The ion–molecule reaction pathways leading from a particular reactant ion to a particular product ion can, in principle, be established from either of two types of double-resonance FT/ICR experiments. First, if a reactant ion is ejected and one or more product ions decrease in abundance, then those products must originate from the ejected reactant. Alternatively, if one reactant ion is isolated (i.e., ions of all other mass-to-charge (m/z) ratios are removed), then any remaining products must originate from the isolated reactant. Both methods have recently been applied to ion–molecule chemistry of transition-metal complexes and clusters.[32-35] We prefer the second method because fewer ions are present, thereby reducing space–charge effects, which can degrade mass resolution.

In order to establish reaction pathways, one must first isolate reagent ions of a given chemical formula, e.g., $H_2Os_3(CO)_7^+$, including all of its component osmium isotopes. For example, the mass range for a particular triosmium dimer multiplet containing six osmium atoms, considering only those isotopic ions whose abundance is ≥1% of that of the most abundant ion of that chemical formula, extends for about 24 amu. Clusters whose chemical formulas differ by one carbonyl are separated by 28 amu. For such a case, a successful double-resonance experiment therefore requires complete ejection of ions separated by about 4 amu from unirradiated ions.

In practice, the difficulty of such mass-selective ejection experiments increases markedly with increasing ionic mass-to-charge ratio (m/z) for two reasons. First, even with perfectly selective ejection, the isotopic multiplets for osmium clusters differing by the mass of one carbonyl ligand begin to overlap significantly for clusters containing greater than or equal to nine osmium atoms. Second, because of the reciprocal relation between m/z and ICR

(34) Freiser, B. S. *Talanta* **1985**, *32*, 697–708.
(35) Buckner, S. W.; Freiser, B. S. *J. Am. Chem. Soc.* **1987**, *109*, 1247–1248.

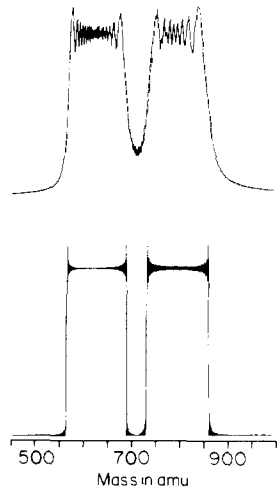

Figure 4. Comparison of selective mass ejection for frequency sweep (top) and SWIFT (bottom) excitation, for equal excitation periods (8.4 ms). Both excitation waveforms were designed to eject all $H_xOs_3(CO)_y^+$ species except for $Os_3(CO)_5^+$. Note the much higher mass selectivity of the SWIFT method.

frequency, the frequency interval between two ions differing by 1 amu in mass decreases with increasing m/z.[20] As shown in Figure 4 (top) for typical experimental conditions, the frequency-domain windowed excitation magnitude spectrum of the ejection pulse produced by a typical time-domain frequency sweep[30,36,37] provides sufficient power for ejection of ions whose masses are higher or lower than that of the targeted ion, but significant excitation power clearly spills over to excite (undesirably) the target ion.

Frequency-sweep ion ejection (Figure 4, top) can be made more selective by increasing the excitation period, but the relatively broad "tails" at the boundaries of the excitation window still intrude at the target ion ICR frequency, with resultant partial ejection of the desired ions. Frequency-sweep ejection of high-abundance ions in the presence of low-abundance ions is particularly difficult. Ion ejection can be made much more selective with SWIFT excitation,[30,31] as seen in Figure 4 (bottom). SWIFT excitation was therefore used for all ejections described below.

Following ion formation and SWIFT excitation designed to eject all but a single triosmium monomer $H_xOs_3(CO)_y^+$ isotopic multiplet and an ion–molecule reaction period of fixed length, broad-band excitation/detection produced each of the series of FT/ICR mass spectra shown in Figure 5. At first glance, the SWIFT isolation of each isotopic multiplet appears imperfect: small peaks corresponding to the four highest mass triosmium monomers are present, as if they were incompletely ejected. However, these peaks disappear when the ion–molecule reaction period is eliminated, showing that the initial SWIFT ejection window is indeed successful in isolating ions of the specified m/z range. It is possible that the "ejected" ions are not completely ejected and slowly find their way back into observable positions in the cell. Unfortunately, even SWIFT ejection is not completely selective, and attempts to increase the ejection power actually make matters worse by decreasing the abundance of the selected ions relative to the unwanted ions. Alternatively, accelerated ions in the process of being ejected may charge transfer to neutral parent molecules to produce $H_2Os_3(CO)_{10}^+$, which in turn may lose a few carbonyls to produce the observed spectrum. So long as the minor triosmium monomer peaks are lower in abundance than the selected ions, the small additional peaks do not interfere with the interpretation of the spectra and can in any case be compensated by subtracting from each triosmium dimer spectrum the dimer spectrum arising from isolation of reactant $H_2Os_3(CO)_{10}^+$ ions.

(36) Comisarow, M. B.; Marshall, A. G. *Chem. Phys. Lett.* **1974**, *26*, 489–490.
(37) Marshall, A. G.; Roe, D. C. *J. Chem. Phys.* **1980**, *73*, 1581–1590.

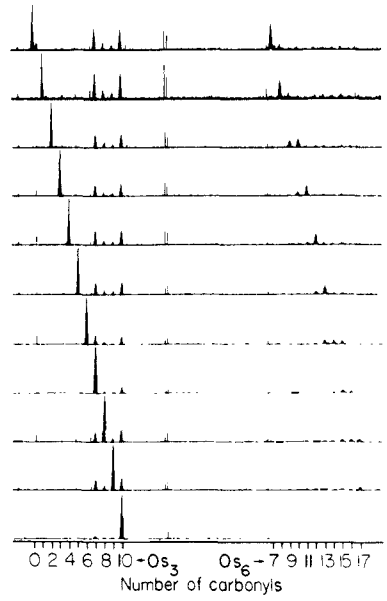

Figure 5. FT/ICR mass spectra of the $H_xOs_3(CO)_y^+$ monomers and $H_aOs_6(CO)_b^+$ dimers, after each monomer has been successively isolated by means of SWIFT excitation and allowed to react with neutral $H_2Os_3(CO)_{10}$. Each mass spectrum is scaled such that the peak for the most abundant ion is at full vertical displacement. Experimental parameters are listed in Table I.

Ionic Products from Self-Reaction of $H_2Os_3(CO)_{10}$ with Its Molecular and Daughter Ions. An obvious feature of Figures 2 and 3 is that the number of osmium atoms in each metal cluster cation is a multiple of 3. Thus, no Os–Os bonds are broken in forming the larger clusters, and the reactions evidently occur by addition accompanied by the elimination of the appropriate numbers of hydrogens and carbonyls. Although the mass spectrum of electron-ionized $Os_3(CO)_{12}$ shows fragments corresponding to loss of 1–10 carbonyls (i.e., all the way down to Os_3^+), no cleavage of the metal–metal bonds is seen. In contrast, metal–metal bonds are readily broken in analogous iron and ruthenium clusters,[33] in accord with the trend of metal–metal bonds to become stronger in proceeding down a column in the periodic table.

Figure 6 shows various $H_xOs_6(CO)_y^+$ triosmium dimer cations ($x = 0, 2$; $7 < y < 18$) formed by self-reaction of $H_2Os_3(CO)_{10}$ with its molecular and fragment ions. Two hydrogens are present in clusters with ≥ 14 carbonyls and are absent for clusters with ≤ 13 carbonyls (see below). Because neutral $Os_6(CO)_{18}$ and $H_2Os_6(CO)_{18}$ are both known, the highest mass triosmium dimer cation might be expected to have one of those chemical formulas. Although detectable, $H_2Os_6(CO)_{18}^+$ ions are low in abundance; the highest mass triosmium dimer with signficant abundance is $H_2Os_6(CO)_{17}^+$.

The triosmium trimer cation region is plotted with expanded mass scale in Figure 7. Although the mass resolution is sufficient to resolve nominal mass differences, the peak height irregularities due to limited signal-to-noise ratio and limited digital resolution (i.e., there may not be a data point close to the maximum of each peak) make determination of the number of hydrogens difficult. Nevertheless, careful scrutiny of the spectrum suggests that the two lowest mass triosmium trimer cations contain eight hydrogens, the next five highest mass cations (two of which are barely visible) contain none, and the four highest cations contain two.

Reaction Pathways. Figure 8 shows a mass scale expansion of the triosmium dimer product ion region of the MS/MS experiment of Figure 5. The products arising from the triosmium monomers up to and including $H_2Os_3(CO)_7^+$ are easily seen, but condensation products from higher mass monomers are low in abundance. $H_2Os_3(CO)_8^+$, $H_2Os_3(CO)_9^+$, and $H_2Os_3(CO)_{10}^+$ all form $H_2Os_6(CO)_{17}^+$, which fragments to its daughter cations. As noted above, the triosmium dimer spectrum resulting from reaction of isolated $H_2Os_3(CO)_{10}^+$ can serve as a reference spectrum for establishing the connections between monomer reactants and dimer

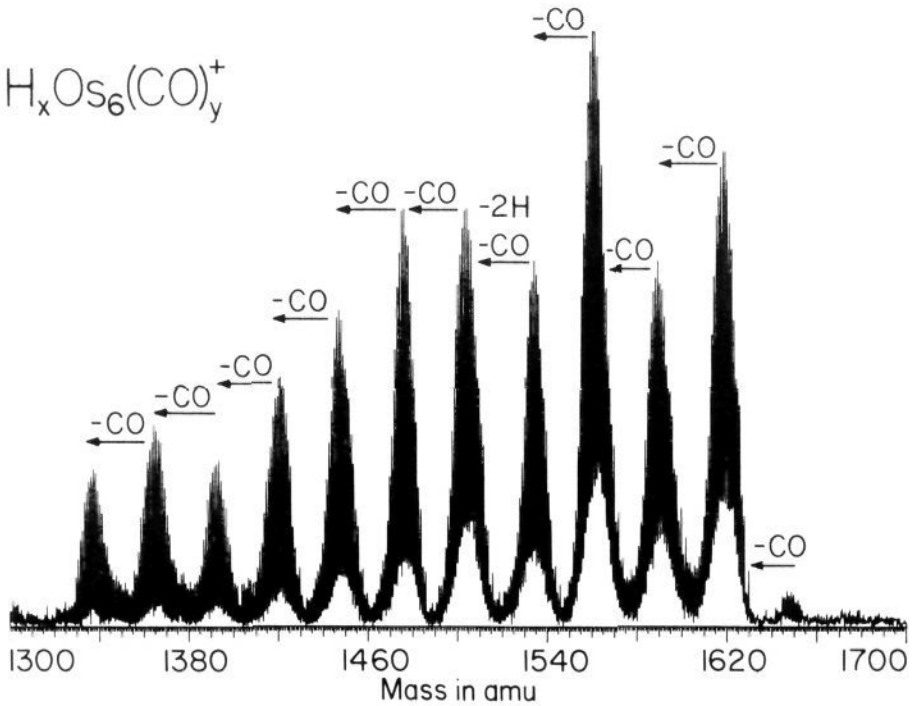

Figure 6. FT/ICR mass spectrum of positive ions formed from the 0.5-s self-reaction of $H_2Os_3(CO)_{10}$ (1×10^{-9} Torr) with its molecular and daughter ions to give species ranging from $Os_6(CO)_7^+$ to $H_2Os_6(CO)_{18}^+$.

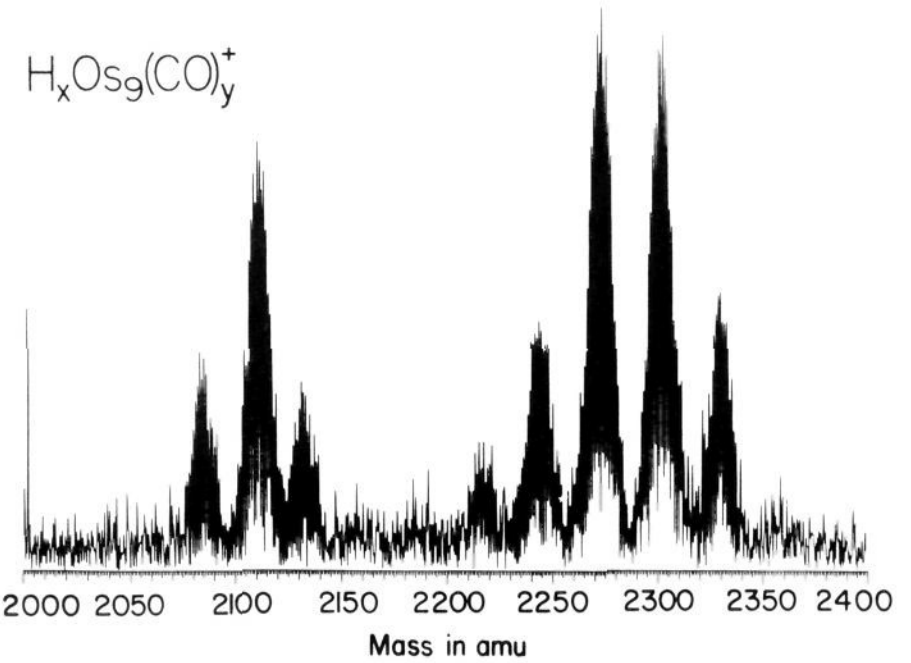

Figure 7. Mass scale expansion of the trimer ion mass spectral region of Figure 3, showing the resolution of the various isotopic mass clusters.

products (except for $H_2Os_6(CO)_{17}^+$, which results from $H_2Os_3(CO)_8^+$ and $H_2Os_3(CO)_9^+$. For example, a comparison of the triosmium dimer spectra (see Figure 8) resulting from reaction of $H_2Os_3(CO)_8^+$ with that of $H_2Os_3(CO)_{10}^+$ shows that $H_2Os_3(CO)_8^+$ produces $H_2Os_6(CO)_{15}^+$, $H_2Os_6(CO)_{16}^+$, and $H_2Os_6(CO)_{17}^+$. Likewise, $H_2Os_3(CO)_9^+$ can be seen to produce $H_2Os_6(CO)_{17}^+$. Table II summarizes the ion–molecule reactions established by SWIFT isolation of successive $H_xOs_3(CO)_y^+$ reactants.

Table II shows that each triosmium dimer ion is formed via several reactions between triosmium monomers and neutrals. Most commonly, two hydrogens are lost, possibly as H_2, along with two or three carbonyls. The loss of two and three carbonyls occurs in the formation of every triosmium dimer, with two exceptions: a loss of two carbonyls cannot occur in the formation of $Os_6(CO)_7^+$, and a loss of three carbonyls does not occur in the formation of $H_2Os_6(CO)_{16}^+$. The overall pattern of results is readily understood from Table III, which lists the branching ratio for each of the dimerization reactions. The pattern across a given row of Table III shows which dimers are formed in what ratio from a particular monomer. The uppermost diagonal in Table III represents all of the reactions in which three carbonyls are lost. The next uppermost diagonal represents reactions in which two carbonyls are lost, and so on. Inspection of the three-carbonyl diagonal shows an essentially monotonic decrease in the ratio of three-carbonyl loss to two-carbonyl loss in proceeding from smaller to larger dimer clusters. Thus, the formation of $H_2Os_6(CO)_{16}^+$ from $H_2Os_3(CO)_9^+$ is not observed. The loss of either one or zero

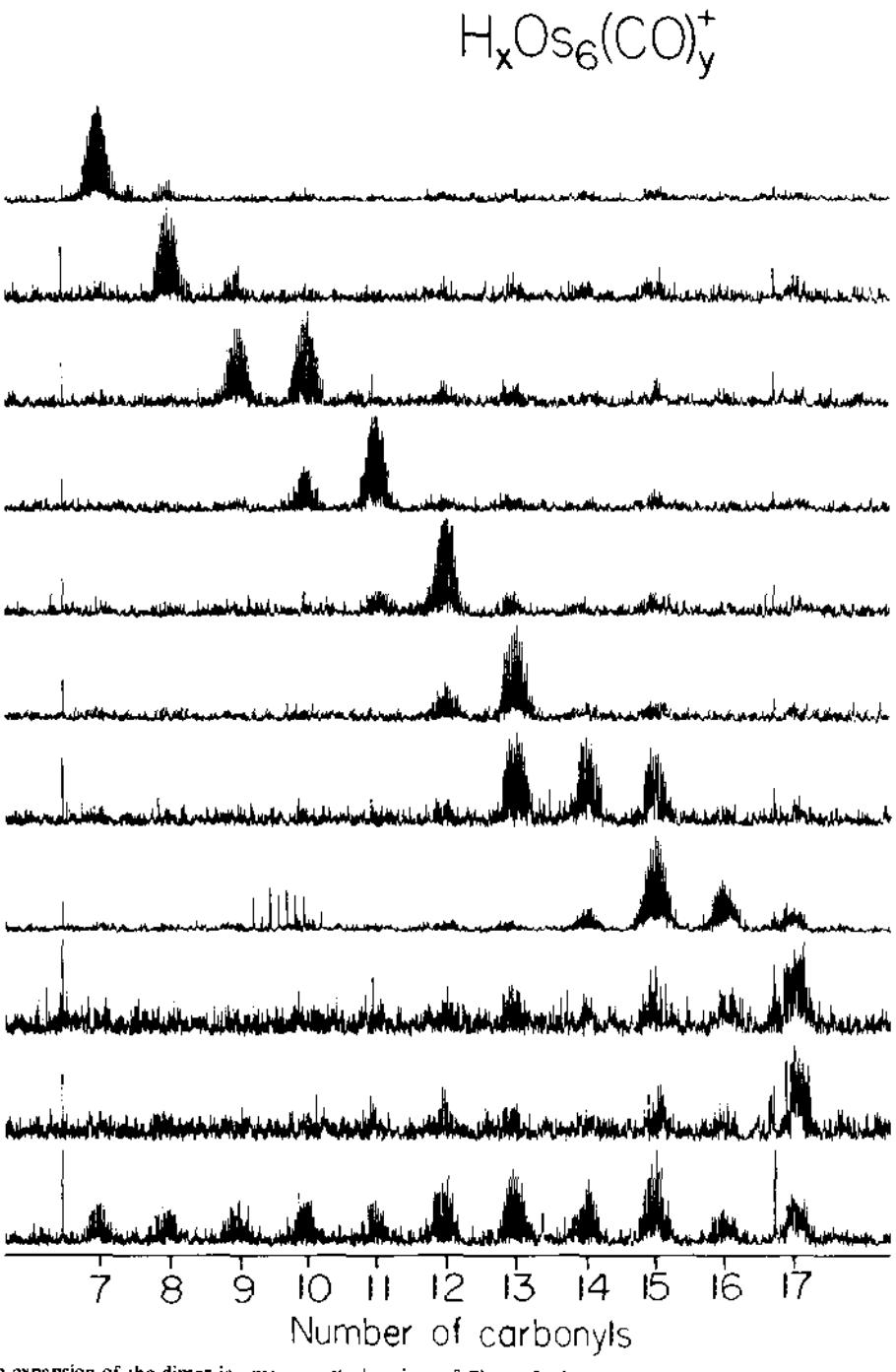

Figure 8. Mass scale expansion of the dimer ion mass spectral regions of Figure 5, showing the resolution of the various isotopic mass clusters.

carbonyls is also seen, but the former occurs only for the three highest mass dimer products [$H_2Os_6(CO)_{15}^+$, $H_2Os_6(CO)_{16}^+$, and $H_2Os_6(CO)_{17}^+$] and the latter occurs only for $H_2Os_6(CO)_{17}^+$.

Reaction pathways for the reactions of triosmium dimer ions with the present triosmium neutral to form triosmium trimers may also be deduced. The most elegant way would be first to allow the dimer ions to form, then isolate one dimer ion by using SWIFT excitation to remove all monomer, trimer, and other dimer ions, and then detect the trimer ions formed after a suitable reaction period. Unfortunately, ions are lost during each stage, and we were unable to produce enough trimer ions by that method. More practically, SWIFT excitation can be used to isolate a particular $H_xOs_3(CO)_y^+$ monomer reagent ion, which will react with $H_2Os_3(CO)_{10}$ to produce one or two $H_aOs_6(CO)_6^+$ dimer species, which in turn will react further with neutral $H_2Os_3(CO)_{10}$ to produce trimers. In particular, the lower mass monomer ions tend to give a single major dimer product ion. In this way, we found that triosmium trimer cations are typically formed from dimer cations with the loss of two to three carbonyls.

Ion–Molecule Reaction Rate Constants. In the present experiments, ion–molecule reactions are expected to exhibit pseudo-first-order kinetics, because neutral molecules are present at a much higher concentration than the ions. Following an initial nonlinear increase in reactant ion concentration during the period in which ions are forming by multiple reactions, a plot of the logarithm of reactant ion concentration vs reaction period indeed shows the straight-line decay expected for a first-order process. Relative ion–molecule reaction rate constants can then be determined from the (negative) slopes of such plots. For cases in which the ion is relatively unreactive, so that its concentration does not yet decay during the available reaction period, a maximum ion–molecule rate constant can be determined from the slope

Table II. Dimerization Reactions of $H_2Os_3(CO)_{10}$ with Its Parent and Daughter Ions

$H_2Os_3(CO)_{10} + H_2Os_3(CO)_{10}^+ \rightarrow H_2Os_6(CO)_{17}^+ + H_2 + 3CO$
$H_2Os_3(CO)_{10} + H_2Os_3(CO)_9^+ \rightarrow H_2Os_6(CO)_{17}^+ + H_2 + 2CO$
$H_2Os_3(CO)_{10} + H_2Os_3(CO)_8^+ \rightarrow H_2Os_6(CO)_{17}^+ + H_2 + CO$
$H_2Os_3(CO)_{10} + H_2Os_3(CO)_7^+ \rightarrow H_2Os_6(CO)_{17}^+ + H_2$

$H_2Os_3(CO)_{10} + H_2Os_3(CO)_8^+ \rightarrow H_2Os_6(CO)_{16}^+ + H_2 + 2CO$
$H_2Os_3(CO)_{10} + H_2Os_3(CO)_7^+ \rightarrow H_2Os_6(CO)_{16}^+ + H_2 + CO$

$H_2Os_3(CO)_{10} + H_2Os_3(CO)_8^+ \rightarrow H_2Os_6(CO)_{15}^+ + H_2 + 3CO$
$H_2Os_3(CO)_{10} + H_2Os_3(CO)_7^+ \rightarrow H_2Os_6(CO)_{15}^+ + H_2 + 2CO$
$H_2Os_3(CO)_{10} + H_2Os_3(CO)_6^+ \rightarrow H_2Os_6(CO)_{15}^+ + H_2 + CO$

$H_2Os_3(CO)_{10} + H_2Os_3(CO)_7^+ \rightarrow H_2Os_6(CO)_{14}^+ + H_2 + 3CO$
$H_2Os_3(CO)_{10} + H_2Os_3(CO)_6^+ \rightarrow H_2Os_6(CO)_{14}^+ + H_2 + 2CO$

$H_2Os_3(CO)_{10} + H_2Os_3(CO)_6^+ \rightarrow Os_6(CO)_{13}^+ + 2H_2 + 3CO$
$H_2Os_3(CO)_{10} + Os_3(CO)_5^+ \rightarrow Os_6(CO)_{13}^+ + H_2 + 2CO$

$H_2Os_3(CO)_{10} + Os_3(CO)_5^+ \rightarrow Os_6(CO)_{12}^+ + H_2 + 3CO$
$H_2Os_3(CO)_{10} + Os_3(CO)_4^+ \rightarrow Os_6(CO)_{12}^+ + H_2 + 2CO$

$H_2Os_3(CO)_{10} + Os_3(CO)_4^+ \rightarrow Os_6(CO)_{11}^+ + H_2 + 3CO$
$H_2Os_3(CO)_{10} + Os_3(CO)_3^+ \rightarrow Os_6(CO)_{11}^+ + H_2 + 2CO$

$H_2Os_3(CO)_{10} + Os_3(CO)_3^+ \rightarrow Os_6(CO)_{10}^+ + H_2 + 3CO$
$H_2Os_3(CO)_{10} + Os_3(CO)_2^+ \rightarrow Os_6(CO)_{10}^+ + H_2 + 2CO$

$H_2Os_3(CO)_{10} + Os_3(CO)_2^+ \rightarrow Os_6(CO)_9^+ + H_2 + 3CO$
$H_2Os_3(CO)_{10} + Os_3(CO)^+ \rightarrow Os_6(CO)_9^+ + H_2 + 2CO$

$H_2Os_3(CO)_{10} + Os_3(CO)^+ \rightarrow Os_6(CO)_8^+ + H_2 + 3CO$
$H_2Os_3(CO)_{10} + Os_3^+ \rightarrow Os_6(CO)_8^+ + H_2 + 2CO$

$H_2Os_3(CO)_{10} + Os_3^+ \rightarrow Os_6(CO)_7^+ + H_2 + 3CO$

of the slowly rising part of the semilog plot before the maximum is reached.

Table IV lists the relative rate constants for the triosmium monomers, dimers, and trimers. Rate constants were not calculated for $H_2Os_6(CO)_{18}^+$, $Os_9(CO)_{16}^+$, $Os_9(CO)_{17}^+$, or $H_2Os_9(CO)_{23}^+$ because of their small abundances. When the 1000-fold difference in pressure is taken into account, the pseudo-first-order rate constants obtained in the present experiments are of the same magnitude as those previously determined for rhenium and manganese compounds.[8,9] In order to analyze the kinetic data, we next need to discuss the relation between electron deficiency and molecular structure.

Electron Deficiency. If each osmium atom is assumed to require 18 valence electrons, the average electron deficiency, ED, of an osmium cluster cation can be computed from[8] eq 1 in which n

$$\mathrm{ED} = \frac{18n - (8n + 2m + 2b + h - 1)}{n} + \frac{2X}{n} \qquad (1)$$

is the number of osmium atoms, m is the number of carbonyls, b is the number of osmium–osmium bonds, h is the number of hydrogens, and 1 is included to account for the single positive charge. X is a factor, proposed by Teo,[38] that takes into consideration the electron delocalization that occurs in large metal clusters. Meckstroth et al.[8,9] showed that, for rhenium and manganese carbonyls, built up in units of two metal atoms each, the self-reaction pseudo-first-order rate constant, k, increases until the average electron deficiency reaches 2. At this point, each metal atom can accept a 2-electron donor, and the rate constant levels off to the collision rate. Meckstroth et al.[8,9] observed a smooth correlation between self-reaction rate constant and electron deficiency for manganese and rhenium cluster cations.

The relative self-reaction rate constants for the triosmium monomers of this study also show a relatively smooth increase with increasing electron deficiency. The rate constants for further self-reaction of the triosmium dimers with triosmium monomer neutrals also increase with increasing electron deficiency, but the maximum reactivity levels off at a rate constant approximately half that of the triosmium monomers. Consideration of the possible ion structures offers insight into these results.

Ion Structure. Triosmium monomer ions are assumed to have the structure of neutral $H_2Os_3(CO)_{10}$: i.e., triangular, with an

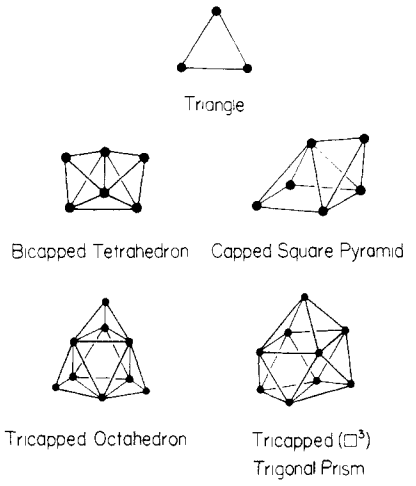

Figure 9. Possible structures (i.e., metal–metal bonds) of triosmium monomers (top), dimers (middle), and trimers (bottom). Carbonyls and hydrogens are not shown.

osmium at each vertex[1] (Figure 9, top row). If this arrangement of osmium atoms is conserved as ligands are successively removed, then the calculated electron deficiency might be expected to change discontinuously on loss of the two hydrogens (see Table IV). Since several previous studies of other transition-metal cluster ions indicate that the pseudo-first-order rate constant for reactant ion disappearance correlates smoothly with electron deficiency,[8,9] one might predict a corresponding discontinuity in rate constant unless a change in structure and/or number of bonds occurs on loss of hydrogens from $H_2Os_3(CO)_6^+$. Table IV shows that, for the $H_xOs_3(CO)_y^+$ ion series, the loss of the two hydrogens occurs after the rate constant has already increased to its maximum value; thus, the proposed discontinuity in rate constant is not experimentally observable. In any case, there is no reason to expect a change in structure of the Os_3 skeleton on loss of two hydrogens. The three osmium atoms must form either a triangle or an open chain. The Os_3 skeleton does not break down in the mass spectrometer, and the first step in a breakdown is a change from a triangular to an open-chain geometry. Moreover, changing from a triangle to an open chain eliminates one metal–metal bond and further increases the electron deficiency.

For the larger osmium cluster cations, we again begin from known structures of closely related neutrals: $H_2Os_6(CO)_{18}$ is a capped square pyramid,[39] whereas $Os_6(CO)_{18}$ is a bicapped tetrahedron.[40] Both structures are shown in the middle row of Figure 9. It should therefore seem reasonable that the triosmium dimer ions containing hydrogen have the former structure and triosmium dimers without hydrogen have the latter structure. The present study provides evidence that this is indeed the case. The two hydrogens are lost from $H_2Os_6(CO)_{14}^+$ just before the rate constant reaches its collision-rate maximum. Thus, if the Os_6 structure is conserved for all $H_xOs_6(CO)_y^+$ species, then a discontinuity in electron deficiency caused by the sudden loss of 2 electrons (from the hydrogens) should be observable as a discontinuous jump in rate constant. However, Figure 10 shows a smooth variation of rate constant with number of carbonyls. Therefore, we propose that the variation in electron deficiency with carbonyl number should also be smooth, namely, by a change in structure from capped square pyramidal to bicapped tetrahedral on loss of the two hydrogens. The additional metal–metal bond in bicapped tetrahedron thus compensates for the loss of the two hydrogens in the electron count.

An alternative mechanism for achieving a smooth variation in electron deficiency on loss of two hydrogens from $H_2Os_6(CO)_{14}^+$ is to introduce an additional Os–Os bond on removal of the two

(38) Teo, B. K. *Inorg. Chem.* **1984**, *23*, 1251–1257.

(39) McPartlin, M.; Eady, C. R.; Johnson, B. F. G.; Lewis, J. *J. Chem. Soc., Chem. Commun.* **1976**, 883–885.

(40) Mason, R.; Thomas, K. M.; Mingos, D. M. P. *J. Am. Chem. Soc.* **1973**, *95*, 3802–3804.

Table III. Branching Ratios for Dimerization Reactions of $H_xOs_3(CO)_y^+$ with $H_2Os_3(CO)_{10}$[a]

no. of carbonyls in monomer cation	no. of carbonyls in dimer cation										
	17	16	15	14	13	12	11	10	9	8	7
10	1.00										
9	1.00	0.00									
8	0.78	0.20	0.02								
7	0.13	0.30	0.50	0.07							
6			0.35	0.39	0.26						
5					0.78	0.22					
4						0.86	0.14				
3							0.70	0.30			
2								0.55	0.45		
1									0.17	0.83	
0										0.15	0.85

[a] Each entry represents the fraction of each monomer ion that reacts with neutral parent to form the dimer ion listed at the top of that column. The rightmost diagonal represents reactions in which three carbonyls are lost, the adjacent diagonal represents loss of two carbonyls, and so on.

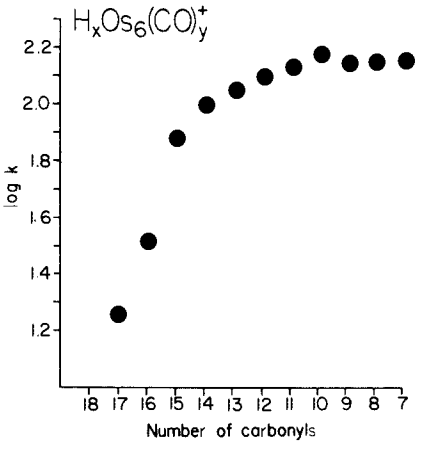

Figure 10. Plot of the logarithm of relative rate constant for disappearance of triosmium dimer ions, $H_xOs_6(CO)_y^+$, vs the number of carbonyls, y.

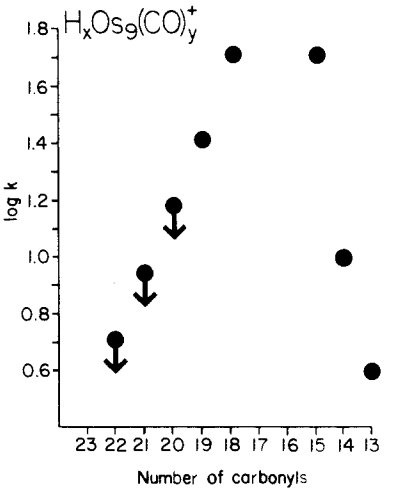

Figure 11. Plot of the logarithm of relative rate constant for disappearance of triosmium trimer ions, $H_xOs_9(CO)_y^+$, vs the number of carbonyls, y. The three leftmost values represent upper limits (see text).

hydrogens to give an Os–Os double bond, thereby increasing the electron count by 2 electrons (see below). However, double bonds are unlikely, since large osmium clusters are not known to contain such bonds. $[Os_9(CO)_{21}(CHC(R)CH)]^-$ (R = Me or Et)[41] was suspected to contain an Os–Os double bond until the length of the bond in question, 2.639 Å, was compared to the shortest known Os–Os single bond, 2.600 Å.

Similar arguments can be advanced to justify a change in structure in triosmium trimers on loss of two hydrogens from $H_2Os_9(CO)_{20}^+$. Figure 11 shows a smooth increase in electron deficiency on loss of carbonyls from $H_xOs_9(CO)_y^+$, extending down to $Os_9(CO)_{15}^+$. Among the closed polyhedral structures listed by Teo et al.,[42] the tricapped ($\square^3$) trigonal prism, the face-sharing bioctahedron, and the tricapped octahedron all have the most metal–metal bonds, thereby minimizing the electron deficiency. However, the face-sharing bioctahedron is not easily built up from the experimentally observed triangular triosmium subunits, leaving the tricapped ($\square^3$) trigonal prism and the tricapped octahedron (Figure 9, bottom row) as likely structures. Therefore, a smooth increase in electron deficiency and rate constant on loss of carbonyls from $H_xOs_9(CO)_y^+$ results if the structure of the triosmium trimer changes from a tricapped ($\square^3$) trigonal prism ($X = 2$ in eq 1) to a tricapped octahedron ($X = 1$ in eq 1) on loss of two hydrogens from $H_2Os_9(CO)_{20}^+$. Unfortunately, no neutral triosmium trimers are known. Jackson et al.[43] have synthesized $[Os_{10}(CO)_{24}C]^{2-}$, which has a tetracapped octahedral structure. That structure is consistent with the proposed tricapped octahedron for $H_2Os_9(CO)_{23}^+$. The only reported Os_9 cluster compound $[Os_9(CO)_{21}(CHC(R)CH)]^-$ (R = Me or Et), synthesized by Johnson et al., has an unusual structure described as "a square pyramid fused at adjacent triangular faces to two trigonal-bipyramidal units."[41]

It should be noted that the two lowest mass triosmium trimers contain eight hydrogens. Since additional hydrogens serve to decrease the electron deficiency, it appears that the triosmium trimer structure does not tolerate an electron deficiency much greater than 2. In support of this view, the small relative rate constants for these two species suggest electron deficiencies even lower than those listed.

From eq 1, a simple calculation shows that a neutral triosmium trimer containing two hydrogens arranged to give a tricapped ($\square^3$) trigonal-prismatic structure would contain 25 carbonyls. However, at most 23 are observed. Possibly the formation of the species containing 24 and 25 carbonyls is kinetically slow and does not occur in the time frame of this experiment, particularly since the highest observed triosmium dimer, $H_2Os_6(CO)_{18}^+$, is of low abundance (see Figure 2). Again, as for the triosmium dimers, the introduction of an Os–Os double bond on loss of two hydrogens from $H_2Os_9(CO)_{20}^+$ offers an alternative but less likely explanation for the smooth increase in electron deficiency on loss of the two hydrogens. For the latter mechanism, all triosmium trimer ions would have the same structure, namely tricapped ($\square^3$) trigonal prismatic or tricapped octahedral.

The difference in relative reactivity between the triosmium monomers and dimers can now be explained by structural arguments. Dimer ions disappear by reacting with neutral monomers to form trimers. The reactants must come together in such a way as to form the bonds required by the trimer. Monomer ions

(41) Johnson, B. F. G.; Lewis, J.; McPartlin, M.; Nelson, W. J. H.; Raithby, P. R.; Sironi, A.; Vargas, M. D. *J. Chem. Soc., Chem. Commun.* **1983**, 1476–1477.

(42) Teo, B. K.; Longoni, G.; Chung, F. R. K. *Inorg. Chem.* **1984**, *23*, 1257–1266.

(43) Jackson, P. F.; Johnson, B. F. G.; Lewis, J.; McPartlin, M.; Nelson, W. J. H. *J. Chem. Soc., Chem. Commun.* **1980**, 224–226.

Table IV. Relative Rate Constants, k (Precise to within Approximately 10%), for Disappearance of $H_xOs_n(CO)_y^+$, n = 3, 6, 9, in the Presence of $H_2Os_3(CO)_{10}$[a]

Os	CO	H	k	proposed ion structure	Os–Os bonds	Teo X	electron deficiency
3	10	2	0.002	triangle	3	0	1.00
3	9	2	0.19	triangle	3	0	1.67
3	8	2	0.13	triangle	3	0	2.33
3	7	2	0.23	triangle	3	0	3.00
3	6	2	0.30	triangle	3	0	3.67
3	5	0	0.29	triangle	3	0	5.00
3	4	0	0.27	triangle	3	0	5.67
3	3	0	0.24	triangle	3	0	6.33
3	2	0	0.26	triangle	3	0	7.00
3	1	0	0.28	triangle	3	0	7.67
3	0	0	0.24	triangle	3	0	8.33
6	18	2		capped square pyramid	11	0	0.17
6	17	2	0.018	capped square pyramid	11	0	0.50
6	16	2	0.032	capped square pyramid	11	0	0.83
6	15	2	0.075	capped square pyramid	11	0	1.17
6	14	2	0.10	capped square pyramid	11	0	1.50
6	13	0	0.11	bicapped tetrahedron	12	0	1.83
6	12	0	0.13	bicapped tetrahedron	12	0	2.17
6	11	0	0.14	bicapped tetrahedron	12	0	2.50
6	10	0	0.15	bicapped tetrahedron	12	0	2.83
6	9	0	0.14	bicapped tetrahedron	12	0	3.17
6	8	0	0.14	bicapped tetrahedron	12	0	3.50
6	7	0	0.14	bicapped tetrahedron	12	0	3.83
9	23	2		tricapped ($\square^3$) trigonal prism	21	2	0.56
9	22	2	<0.005	tricapped ($\square^3$) trigonal prism	21	2	0.78
9	21	2	<0.009	tricapped ($\square^3$) trigonal prism	21	2	1.00
9	20	2	<0.015	tricapped ($\square^3$) trigonal prism	21	2	1.22
9	19	0	0.026	tricapped octahedron	21	1	1.44
9	18	0	0.051	tricapped octahedron	21	1	1.67
9	17	0		tricapped octahedron	21	1	1.89
9	16	0		tricapped octahedron	21	1	2.11
9	15	0	0.051	tricapped octahedron	21	1	2.33
9	14	8	0.010	tricapped octahedron	21	1	1.67
9	13	8	0.004	tricapped octahedron	21	1	1.89

[a] Electron deficiencies were computed from eq 1 for the number of Os–Os bonds and Teo parameter, X, corresponding to each proposed ion structure.

disappear by reacting with neutral monomers to form dimers. In this case the reactants must also come together with a particular relative orientation, but the neutral can approach from either side of the ion rather than from only one direction. Thus, one would predict that the relative rate constants for the triosmium monomers should be twice those of the dimers. Furthermore, it is reasonable that similar orientational restrictions should reduce the rate constant even further as the size of the cluster increases.

Conclusions

FT/ICR experiments at $<10^{-8}$ Torr are shown to be uniquely suited for study of trapped ions formed by electron ionization of thermally labile low-volatility ($<10^{-6}$ Torr) osmium clusters. Isolation of component high-mass ions of a given chemical formula by means of SWIFT excitation is demonstrated to be the method of choice for establishing ion–molecule reaction pathways and kinetics of high-mass ions.

With these techniques, gas-phase polymerization reactions of $H_2Os_3(CO)_{10}$ with its electron-ionized parent and daughter fragment cations have been shown to occur with the elimination of two and three carbonyls. For triosmium dimers and trimers, the relative rate constants for the ion–molecule condensation reactions imply a difference in structure and/or bonding between species having zero or two hydrogens, resulting in a smooth increase in the electron deficiency and relative rate constant on loss of the hydrogens. On the basis of the structures of neutral $H_2Os_6(CO)_{18}$ and $Os_6(CO)_{18}$, triosmium dimers containing hydrogen are assigned a capped square-pyramidal structure, and those without hydrogen, a bicapped tetrahedral structure. A tricapped ($\square^3$) trigonal-prismatic structure is suggested for triosmium trimers containing two hydrogens and $\geq$20 carbonyls, and a tricapped octahedral structure, for trimers with 15–19 carbonyls. An electron deficiency much greater than 2 is avoided by the trimers and is lowered by the addition of hydrogens and possibly by the formation of Os–Os double bonds.

Acknowledgment. We thank S. G. Shore for helpful discussions and for providing $H_2Os_3(CO)_{10}$. We also thank Ling Chen for assisting with Figure 7. This work was supported by grants (to A.G.M.) from the National Science Foundation (CHE-8617244), the U.S. Public Health Service (GM-31683), and The Ohio State University.

Registry No. $H_2OS_3(CO)_{10}^+$, 112270-24-3.